Experimental Investigation on the APR1400 In-Core Instrumentation Penetration Failure

Sang Mo An [a*], Jaehoon Jung [a], Hwan Yeol Kim [a]
[a]*Korea Atomic Energy Research Institute (KAERI), 989-111 Daedeok-daero, Yuseong-gu, Daejeon, Korea*
[*]*Corresponding author: sangmoan@kaeri.re.kr*

1. Introduction

For Korean PWRs (pressurized water reactors), there are many bottom-up type ICI (in-core instrumentation) nozzles which are installed at the reactor lower head (45 for OPR1000 and 61 for APR1400) [1]. The ICI nozzle consists of one pair of K-type thermocouple to measure CET (core exit temperature) and five SPNDs (self-powered neutron detectors) with one background detector to monitor neutron flux [2]. It is noted that they are attached to the inside of the reactor vessel lower head by a partial weld [3]. Therefore, the research on the penetration failure is of importance, as it could lead to melt discharge into the containment and subsequent accident progressions such as corium-concrete interaction and release of a mixture of fission products, combustible gases, and steam into the containment. Consequently, it can lead to a failure of containment due to pressurization and subsequent release of radioactive materials to the environment [4].

A schematic of the APR1400 ICI nozzle at the center of the reactor lower head is given in Fig. 1. The reactor vessel material is SA508, Grade 3, Class 1, and its thickness is 180.6 mm (reactor vessel 175 mm and cladding 5.6 mm). The penetration tube material is Inconel-690, which is installed by boring a vertical hole into the reactor vessel, inserting the tube through the hole, and welding the tube to the vessel inner surface. The weld materials are Inconel Welding Electrode 152 (ENiCrFe-7) for shielded metal arc welding and Inconel Filler Metal 52 (ERNiCrFe-7) for gas tungsten arc welding [5]. They are generally used in nuclear power plants as the Inconel-690 welding materials [6, 7]. A vertical length of the weld is 43 mm. The tube outer diameter at the weld is 76.20 mm but its length depends on the installation positions at the reactor lower head. To facilitate the insertion of the penetration tube into the vessel hole, a gap between the tube outer diameter (76.20 mm) and the vessel hole diameter (76.30 mm) is set to 50 μm. A thimble tube in the penetration tube has the dimensions of 8.94 mm in inner diameter and 11.43 mm in outer diameter. An annulus (19.05 mm in diameter) between the penetration tube and thimble tube is filled with RCS (reactor cooling system) water at system pressure. An ICI assembly is inserted into the thimble tube which is filled with containment air at atmospheric pressure. Therefore, if in-vessel penetration failure occurs during a severe accident, there are two paths available for melt flow: RCS water-filled annulus outside the thimble tube and air-filled channel inside the thimble tube [4].

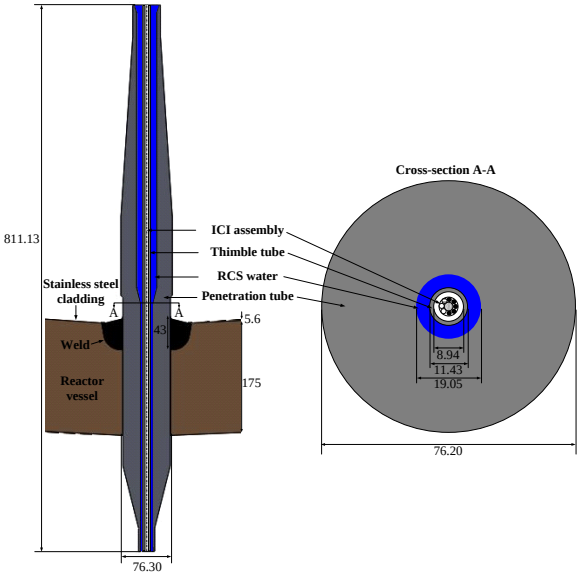

Fig. 1. Configuration of the APR1400 ICI nozzle

The penetration failure mechanism can be divided into two categories; tube ejection out of the reactor lower head and tube rupture outside the vessel [1, 4, 8]. Tube ejection begins with degrading the penetration tube weld strength to zero as the weld is exposed to temperatures as high as its melting point, which is called weld failure, and then overcoming any binding force in the hole of the vessel wall that results from differential thermal expansion of the tube and vessel materials. Tube rupture assumes that the debris bed has melted the penetration tube inside the vessel and melt migrates down into the tube to a location outside the vessel wall where a pressure rupture can occur, thus breaching the pressure boundary.

This paper focuses on the experimental investigation on the tube ejection failure during a severe accident for the APR1400 ICI penetration, as it is exposed to high temperature of melt and the force exerted by the RCS pressure. An APR1400 ICI penetration specimen was provided by Doosan Heavy Industry and ZrO_2 was used as a prototypic melt. During the interaction of the penetration specimen with the melt, the temperature distributions at the reactor vessel, reactor vessel hole and penetration nozzle were monitored to estimate the weld failure and subsequent tube ejection possibilities. After the experiment, the configuration of the penetration specimen was investigated to evaluate the failure progression.

2. Experimental Methods

2.1 Experimental Setup

An experimental facility consists of a furnace vessel, a melt delivery channel and an interaction vessel, as shown in Fig. 2. The VESTA (Verification of Ex-vessel corium STAbilization) facility is a furnace vessel where melt is generated in a melt crucible by induction heating [9, 10]. An interaction crucible is installed in the interaction vessel to perform the penetration failure experiment and simulate RCS pressure condition during a severe accident. A melt delivery channel is connected between the furnace and interaction vessels for stable melt delivery into the interaction crucible.

It is noted that the melt generation and penetration failure experiment was performed simultaneously in the interaction crucible without melt delivery. The interaction crucible is charged with melting materials, and then melt is generated by induction heating by supplying an electrical power with high frequency to the induction coil. The melt temperature is measured by an optical pyrometer on the top of the interaction vessel. During the whole process, argon gas or air is purged through a tube between the interaction crucible and the optical pyrometer to secure the optical path by removing aerosols produced during the melt generation and also to pressurize the space above the pressure boundary as shown in Fig. 2. Two CCD cameras are installed to observe the melt generation process and tube ejection phenomenon.

An ICI penetration specimen is installed at the bottom of the interaction crucible so that it is heated during the melt generation. Figure 3 shows the configuration of the penetration specimen and the temperature measuring points. The weld region is enlarged in the top right-hand corner. The APR1400 ICI penetration specimen was manufactured by a Korean vendor (i.e., Doosan Heavy Industry) according to the real manufacturing process with the same materials and dimensions. The diameter of the reactor vessel including one ICI nozzle was determined to be 250 mm. Based on the analysis of melt composition by SCDAP/RELAP5 and MAAP4, the extruded part of the penetration tube above the inner surface of the reactor vessel was cut to be 30 mm long. Three holes were made in the reactor vessel (RV), near the reactor vessel hole (RVH) and in the penetration tube (P) for inserting Inconel-690 rods. Eleven K-type thermocouples are embedded in each rod to measure the temperature distributions along the vertical direction. RV1-RV10 indicate the temperatures in the reactor vessel, RVH1-RVH7 near the reactor vessel hole, PW8-PW11 in the penetration weld, P1-P11 in the penetration tube. K11 and C11 are positioned just above the surface of the penetration specimen, thus they indicate the melt temperature at that location. Each symbol for the temperature measurement point is labeled with the numbers from the bottom of the reactor vessel. Thus, the same numbers imply the measuring points with the same height.

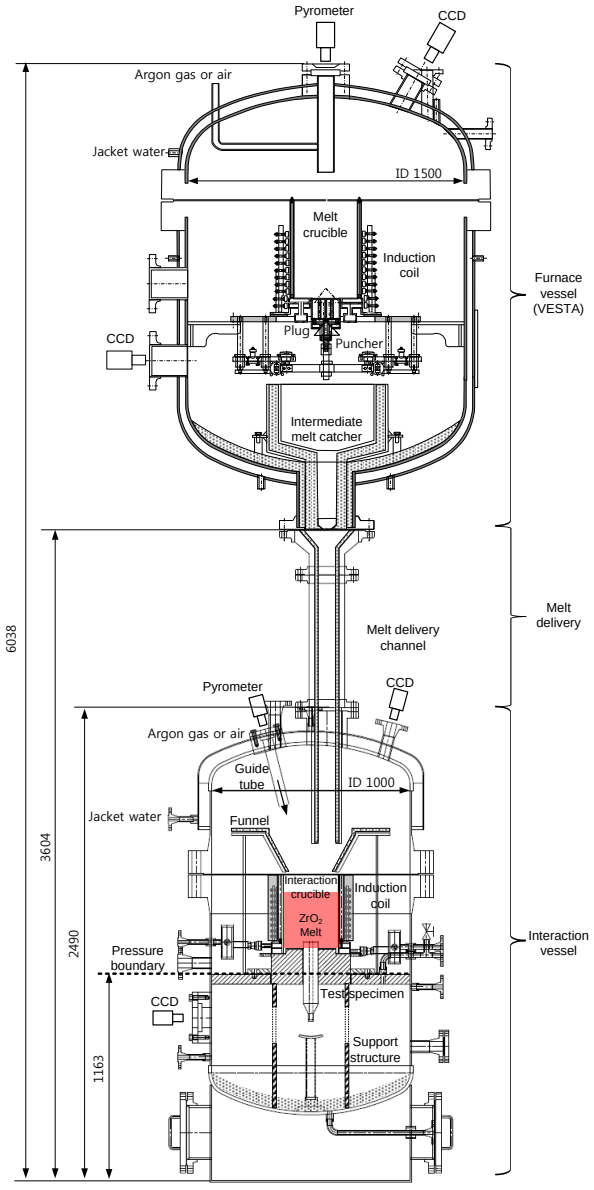

Fig. 2. VESTA Experimental facility

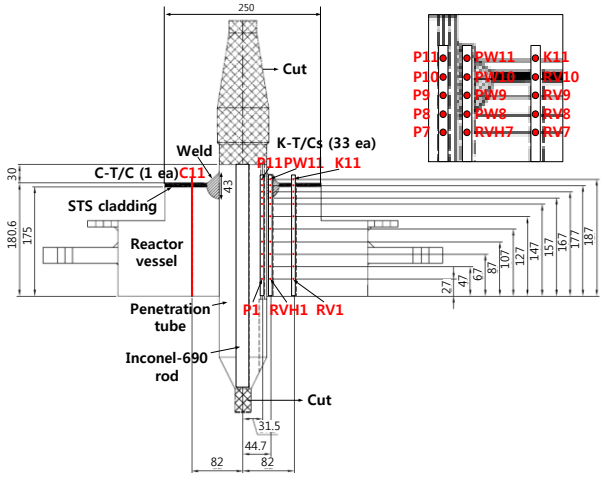

Fig. 3. Configuration of an APR1400 ICI penetration specimen

2.2 Experimental Conditions

ZrO_2 powder (40.94 kg) was used as a melting material and Zr metal ring (0.24 kg) was used as an initiator for induction heating. They were charged on the penetration specimen in the interaction crucible. Figure 4 shows the installation configuration of the penetration specimen with the interaction crucible and a charging pattern of the melting materials. Three holes were made to remove gas during the melt generation and measure the melt temperature by an optical pyrometer.

For the penetration tube to be ejected after the weld failure, the penetration tube needs to be pushed to overcome the binding force in the reactor vessel hole which is induced by differential thermal expansion of the tube and vessel materials. Thus, as the weld temperature increased up to its melting point, the injection and discharge gas flow rates were controlled to pressurize the space above the penetration specimen up to 2.5 bar.

3. Results and Discussion

3.1 Melt Generation

Figure 5 shows the melt generation process along with the supplied electrical power. The electrical power was increased gradually up to 225 kW for stable melt generation. A Q-factor is a measure for the coupling of melt and induction heating. That is, Q-factor decreases as the amount of melt increases. The melt temperature measured by an optical pyrometer began to appear at 1500 s, and the Q-factor showed a sudden decrease at the same time. As the melt temperature increased above

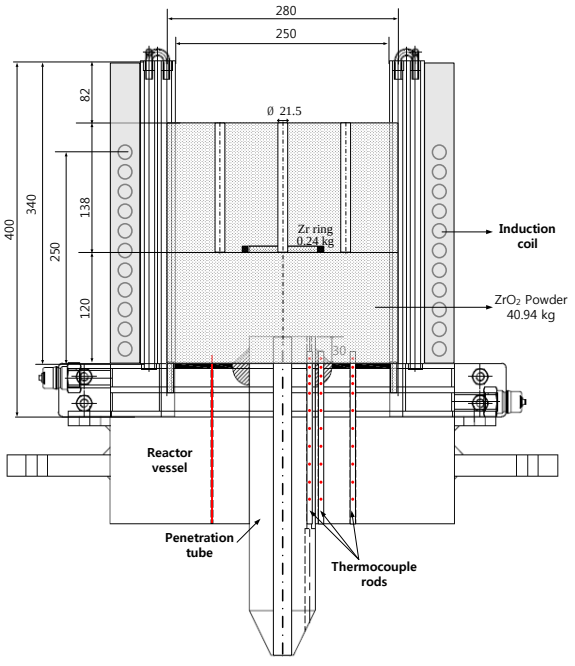

Fig. 4. A charging pattern of melting materials in the interaction crucible

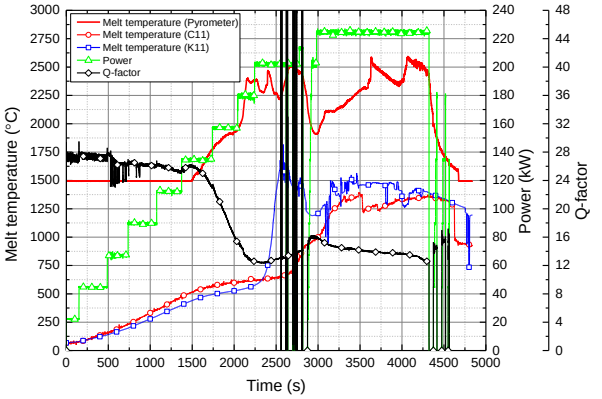

Fig. 5. Melt generation process along with the supplied power in the interaction crucible

2000 ℃, C11 and K11 indicated an increase higher than 1400 ℃, which means that the melt temperature near the surface of the penetration specimen reached around 1400 ℃. Most of the thermocouple readings in the penetration specimen increased high enough to induce weld failure and subsequent tube ejection, and thus we stopped the power supply and terminated the experiment.

3.2 Penetration Heat-up and Failure

Figures 6-9 show the thermocouple readings in the penetration weld (PW), penetration tube (P), the reactor vessel (RV) and reactor vessel hole (RVH). The pressure acting on the penetration specimen was also given in those figures.

As shown in Fig. 6, the weld temperatures (PW8-PW11) showed higher than 1400 ℃ and then a meaningless signal due to the thermocouple failure. In addition, the temperatures at the upper part of the penetration tube (P8-P11) and reactor vessel (RV8-RV10) reached nearly 1400℃ - 1500℃ as shown in Figs. 7 and 8. The melting temperatures for the materials of the penetration tube (Inconel-690) and the reactor vessel (SA508, Grade 3, Class 1) are known as 1343 ℃ - 1377 ℃ [11] and 1461 ℃ - 1501 ℃, respectively. Even though the melting temperature of weld is not available in the literature, it can be assumed

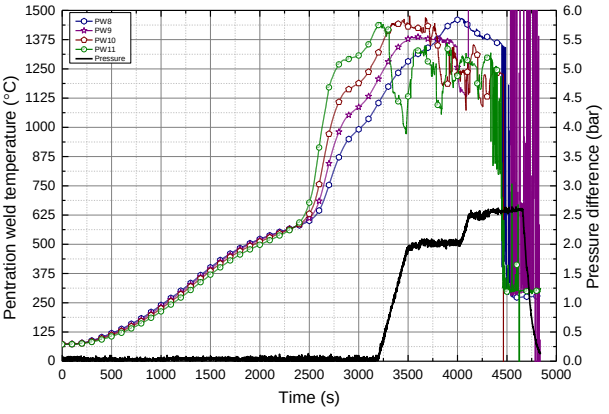

Fig. 6. Temperature distribution in the penetration weld

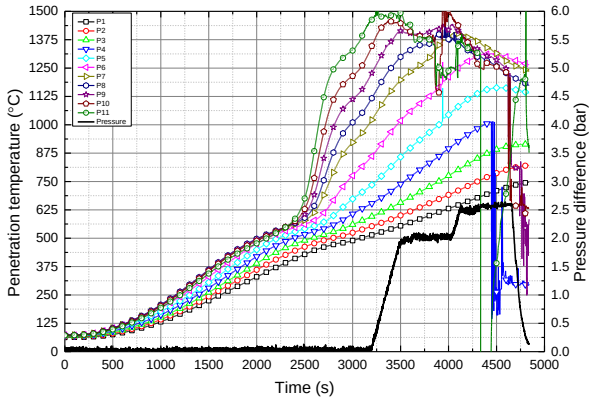

Fig. 7. Temperature distribution in the penetration tube

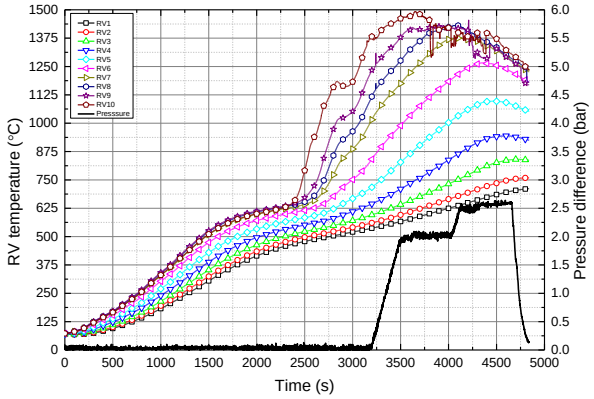

Fig. 8. Temperature distribution in the reactor vessel

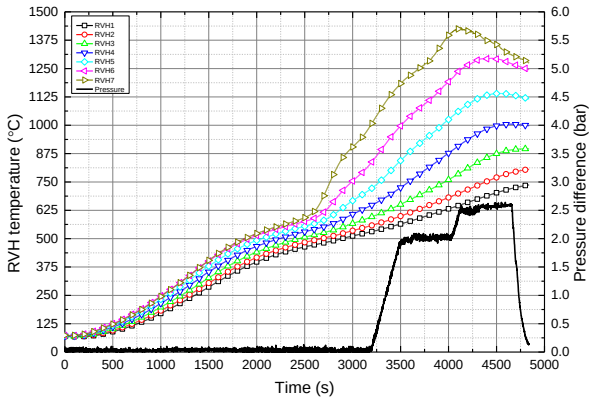

Fig. 9. Temperature distribution near the reactor vessel hole

to be similar to that of Inconel-690. Therefore, it was estimated that the upper parts of the penetration tube and the reactor vessel with stainless steel cladding were ablated severely, which resulted in the weld failure. When the weld temperatures reached higher than 1000 ℃, the penetration tube started to be pushed by increasing the pressure above the penetration specimen. It was maintained at about 2 bar and 2.5 bar for a few hundred seconds. However, even though it was estimated that the penetration specimen was damaged seriously under the pressurized condition, the penetration tube ejection did not occur in the end.

3.3 Observation of the Penetration Specimen

The top surface images of the penetration specimen before and after the experiment are compared in Fig. 10. As predicted previously, the extruded part of the penetration tube on the surface of the specimen was ablated completely.

The cross-sectional image of the specimen is given in Fig. 11, where it is compared with the original configurations before the experiment (a black line) for the reactor vessel, cladding, penetration tube and weld. Nitric acid was applied to the cutting surface to distinguish the reactor vessel from other materials. The reactor vessel (carbon steel) is corroded easily by acid while the penetration tube, weld and stainless steel cladding (Ni-Cr based alloys) are not. As shown in Fig. 11, the upper part of the cross-section is shinny while the lower part appears a brown color due to corrosion. The region in the red-dotted line corresponds to the reactor vessel before the experiment. Thus, if the reactor vessel had been intact, the region would have appeared a brown color. Therefore, it is estimated that the melt mixture of the penetration tube, weld and stainless steel cladding penetrated into the red-dotted region. However, further investigation on the chemical composition for the failed region and precision measurement for the gap between the penetration tube and the reactor vessel hole is necessary to understand the overall penetration failure process and find the experimental conditions for the tube ejection failure.

(a) (b)

Fig. 10. Comparison of the surface image of the penetration specimen before (a) and after the experiment (b)

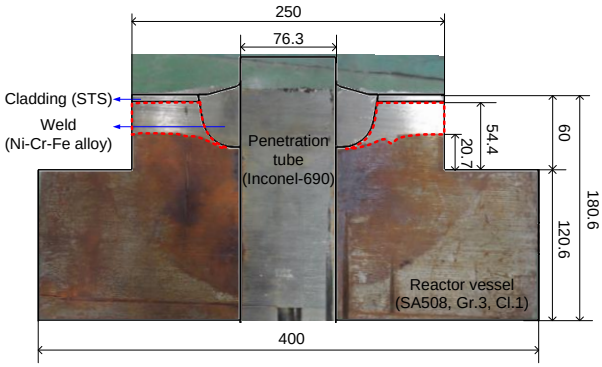

Fig. 11. Cross-section of the penetration specimen before and after the experiment

4. Conclusions

The tube ejection failure experiment was performed for the APR1400 in-core instrumentation penetration nozzle. For the verification experiment during a severe accident, the APR1400 ICI penetration specimen was manufactured according to the real manufacturing process with the same materials and dimensions. Zirconium dioxide was used as a simulant of corium melt and interacted with the penetration specimen. The specimen was pressurized up to 2.5 bar during the interaction with melt to induce the tube ejection. The penetration weld was heated up to its melting temperature, and the penetration tube and weld above the reactor vessel surface were eroded severely by the melt. However, even though it was estimated that the weld failure occurred and the reactor vessel with stainless cladding was ablated severely by the melt, the tube ejection phenomenon was not observed and consequently the integrity for the APR1400 ICI penetration was confirmed in the present experimental conditions.

The final goal of this research is to improve the penetrations failure models in MAAP5 codes and improve the models based on the experimental results. To achieve this goal, it is necessary to find the conditions of the melt temperature and pressure acting on the penetration tube for the tube ejection failure. Therefore, the heat flux and pressure on the penetration tube need to be increased.

The penetration failure experiments will be performed by adopting the melt delivery method because it is a more realistic situation during a severe accident. In addition, the experiments in the ex-vessel reactor vessel cooling condition will be performed also because the IVR (in-vessel melt retention) by ex-vessel reactor vessel cooling has been adopted for the APR1400.

ACKNOWLEDGMENTS

This work was supported by the National Research Foundation of Korea (NRF) grant funded by the Korea government (MSIP) (No. 2012M2A8A4025885).

REFERENCES

[1] S. M. An and H. Y. Kim, Revisit of Penetration Failure Models and Calculations for APR1400 ICI Penetrations, Proceedings of Korean Nuclear Society Autumn Meeting, Oct. 24-25, 2013, Gyeongju, Korea.
[2] D. Shin, M. Chae, S. Kim, K. Lee and S. H. Ye, Studies of Behavior Melting Temperature Characteristics for Multi Thermocouple In-Core Instrument Assembly, Proceedings of Korean Nuclear Society Spring Meeting, May 7-8, 2015, Jeju, Korea.
[3] S. M. An, J. Jung, K. S. Ha and H. W. Kim, Experimental Investigation on APR1400 In-Core Instrumentation Penetration Failure during a Severe Accident, Proceedings of International Congress on Advances in Nuclear Power Plants (ICAPP-2015), May 3-6, 2015, Nice, France.
[4] J. L. Rempe, S. A. Chavez, G. L. Thinnes, G. M. Allison, G. E. Korth, R. J. Witt, J. J. Sienicki, S. K. Wang, L. A. Stickler, C. H. Heath and S. D. Snow, Light Water Reactor Lower Head Failure Analysis, NUREG/CR-5642, 1993.
[5] K. Y. Lee, J. K. Park, C. S. Han et al., Development of Core Technology for KNGR System Design, KAERI/RR-2230, 2001.
[6] T. Matsuoka, H. Yamaoka, K. Hirano and T. Hirano, Development of Welding Methods for Dissimilar Joint of Alloy 690 and Stainless Steel for PWR Components, IHI Engineering Review, Vol. 45, No. 2, p. 39, 2013.
[7] R. R. Shen, Z. Zhou, P. Liu and G. Chai, Effects of PWHT on the Microstructure and Mechanical Properties of ERNiCrFe-7 All-Weld Metal, Welding in the World, Vol. 59, p. 317, 2015.
[8] MAAP(Modular Accident Analysis Program)5, User's Manual, Rev.0, Fauske & Associates, 2008.
[9] S. M. An, K. S. Ha, B. T. Min, S. H. Hong and H. Y. Kim, Experimental Study on the Molten Corium Interaction with Structure by Induction Heating Technique, Proceedings of Korean Nuclear Society Spring Meeting, May. 29-30, 2014, Jeju, Korea.
[10] S. M. An, K. S. Ha, B. T. Min, H. Y. Kim and J. H. Song, Ablation Characteristics of Special Concrete due to an Impinging Zirconium-dioxide Melt Jet, Nuclear Engineering and Design, Vol. 284, p. 10, 2015.
[11] http://www.specialmetals.com/documents/Inconel%20alloy%20690.pdf